Supporting Information

π-Conjugated Redox-active Two-dimensional Polymers as Organic Cathode Materials

Zexin Jin,*[,†,a] Qian Cheng,[†,a] Austin M. Evans,[a] Jesse Gray,[a] Ruiwen Zhang,[b] Si Tong Bao,[a] Fengkai Wei,[b] Latha Venkataraman,[a,b] Yuan Yang,*[,b] Colin Nuckolls*[,a]

[a]Department of Chemistry, Columbia University, New York, New York 10027, United States.
[b]Department of Applied Physics and Applied Mathematics, Columbia University, New York, New York 10027, United States.

*zj2286@columbia.edu
*yy2664@columbia.edu
*cn37@columbia.edu

Table of Contents

1. General Information

Materials. All chemicals were obtained from commercial sources and used as received unless otherwise noted. Suzuki reactions were performed using flame-dried glassware under an atmosphere of nitrogen with dry tetrahedron furan. Super P carbon (C65, Imerys Graphite& Carbon) and poly(vinylidene fluoride) (PVDF) (Kynar Flex) were dried overnight in a vacuum oven at 60 °C and stored in a desiccator. **S1**[1] was synthesized was prepared according to literature procedures.

NMR. Solution-state ^{1}H and ^{13}C NMR spectra were recorded on a Bruker 400 MHz, 500 MHz spectrometer. Chemical shifts for protons are reported in parts per million downfield from tetramethylsilane and are referenced to residual protium within the NMR solvent (C_2DHCl_4: δ 6.00). Chemical shifts for carbon are reported in parts per million downfield from tetramethylsilane and are referenced to the carbon resonances of the solvent ($C_2D_2Cl_4$: δ 74.20). Data are represented as follows: chemical shift, multiplicity, (s = singlet, d = doublet, t = triplet, m = multiplet, b = broad, bm = broad multiplet), coupling constants in hertz, and integration.

MALDI-TOF. The mass spectroscopic data were obtained at the Columbia University mass spectrometry facility using a Bruker ultrafleXtreme MALDI TOF/TOF with a frequency-tripled Nd:YAG laser (355 nm).

Thermogravimetric Analysis (TGA): TGA traces were collected on a TA Instruments TGA Q500 under nitrogen.

Fourier Transform Infrared Spectroscopy (FT-IR): IR spectra were collected on a Perkin Elmer Spectrum 400 FT-IR.

Scanning Electron Microscopy: Scanning electron micrographs were collected using a ZEISS Sigma FE-SEM.

Powder X-Ray Diffraction (PXRD): The powder X-ray diffraction (PXRD) patterns were measured on a PANalytical XPert3 Powder X-ray diffractometer, on a rotating Si zero-background plate.

N_2 Adsorption Isotherm: N_2 adsorption isotherms were collected on a Micromeritics ASAP 2020 HV BET Analyzer. Surface area was calculated using the Brunauer–Emmett–Teller (BET) method. Pore size distributions were calculated from N_2 adsorption isotherms using the cylindrical NLDFT method.

Elemental Analysis: Elemental analyses were tested by Robertson Microlit Laboratories.

2. Synthetic Procedures

2.1 Synthesis of PDI-DA

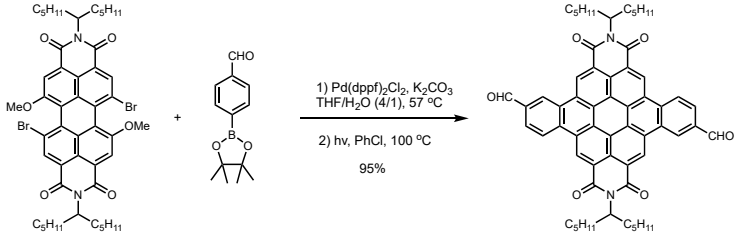

***trans*-Perylene diimide dibenzoaldehyde (PDI-DA):** To a vial was added **S1** (200 mg, 0.218 mmol), 4-formylphenylboronic acid pinacol ester (111 mg, 0.480 mmol), $Pd(dppf)Cl_2$ (16 mg, 0.022 mmol), and potassium carbonate (361 mg, 2.62 mmol). The headspace of the vial was evacuated under vacuum and backfilled with nitrogen three times. Air-free THF/H_2O (v/v, 4:1, 8 ml) solution was then added to the reaction vessel via syringe under nitrogen gas flow, which was sealed with a Teflon cap. The solution was stirred at 57 °C for 12 hours. The reaction was then cooled to room temperature and passed through a silica pad. The solution was concentrated in vacuo and the residue was added 250 ml chlorobenzene. The tube was sealed and placed into a pristine oil bath heated at 100 °C, which was irradiated by four 150 W white LED lights for 12 hours. The reaction mixture was concentrated in vacuo, and the residue was added 50 ml methanol. The solid was collected by filtration and washed with methanol to obtain **PDI-DA** as an orange solid (187 mg, 95% yield).

^{1}H NMR (500 MHz, $C_2D_2Cl_4$) δ 10.67 (s, 2H), 10.43 (d, J = 11.6 Hz, 4H), 9.87 (s, 2H), 9.58 (d, J = 8.6 Hz, 2H), 8.74 (d, J = 8.5 Hz, 2H), 5.65 – 5.43 (m, 2H), 2.68 – 2.45 (m, 4H), 2.22 (td, J = 8.7, 4.3 Hz, 4H), 1.72 – 1.35 (m, 24H), 0.95 (t, J = 7.2 Hz, 12H). ^{13}C NMR (101 MHz, $C_2D_2Cl_4$) δ 191.63, 164.80, 136.39, 133.50, 129.70, 128.78, 128.31, 128.18, 127.54, 126.89, 126.50, 125.94, 124.72, 123.13, 122.81, 55.99, 32.96, 32.04, 27.10, 22.79, 14.23. MALDI-TOF MS: m/z calculated for $C_{60}H_{58}N_2O_6$ [M^-]: 902.4295; found: 902.4597.

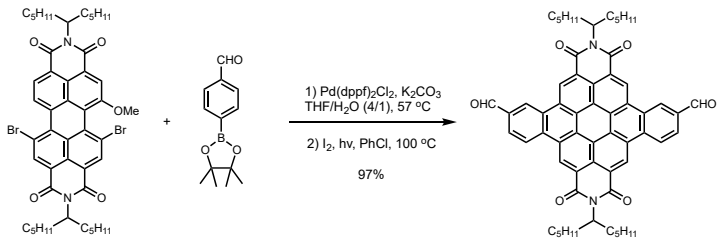

***cis*-Perylene diimide dibenzoaldehyde (*cis*-PDI-DA):** To a vial was added **S2** (100 mg, 0.113 mmol), 4-formylphenylboronic acid pinacol ester (65 mg, 0.28 mmol), Pd(dppf)Cl_2 (8 mg, 0.011 mmol), and potassium carbonate (187 mg, 1.36 mmol). The headspace of the vial was evacuated under vacuum and backfilled with nitrogen three times. Air-free THF/H_2O (v/v, 4:1, 5 ml) solution was then added to the reaction vessel via syringe under nitrogen gas flow, which was sealed with a Teflon cap. The solution was stirred at 57 °C for 12 hours. The reaction was then cooled to room temperature and passed through a silica pad. The solution was concentrated in vacuo and the residue was added 250 ml chlorobenzene and I_2 (50 mg, 0.2 mmol). The tube was sealed and placed into a pristine oil bath heated at 100 °C, which was irradiated by four 150 W white LED lights for 12 hours. The reaction mixture was concentrated in vacuo, and the residue was added 20 ml methanol. The solid was collected by filtration and washed with methanol to obtain *cis*-**PDI-DA** as an orange solid (100 mg, 97% yield).

^{1}H NMR (400 MHz, $C_2D_2Cl_4$) δ 10.67 (s, 2H), 10.43 – 10.29 (m, 4H), 9.84 (s, 2H), 9.53 (d, J = 8.7 Hz, 2H), 8.73 (d, J = 8.6 Hz, 2H), 5.58 – 5.43 (m, 2H), 2.55 (td, J = 9.0, 5.0 Hz, 4H), 2.23 (dd, J = 9.7, 4.5 Hz, 4H), 1.81 – 1.39 (m, 24H), 0.96 (t, J = 7.2 Hz, 12H).^{13}C NMR (101 MHz, $C_2D_2Cl_4$) δ 191.39, 164.45, 136.17, 133.11, 129.34, 128.46, 128.05, 127.65, 127.36, 126.68, 125.80, 125.62, 125.20, 125.01, 124.57, 124.06, 122.68, 122.29, 55.79, 32.74, 31.87, 26.95, 22.61, 14.06. MALDI-TOF MS: m/z calculated for $C_{60}H_{58}N_2O_6$ [M^-]: 902.4295; found: 902.4871.

2.2 Synthesis of model compound

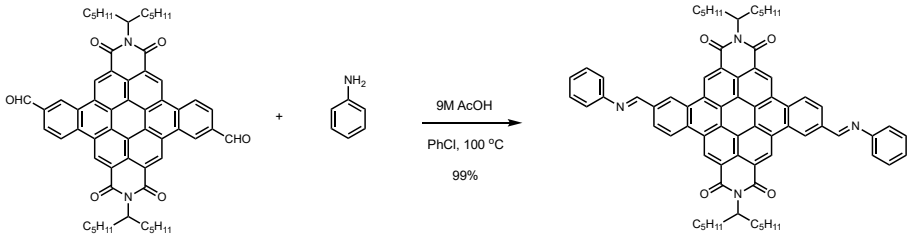

PDI-DA S3 S4

S4: To a vial was added **PDI-DA** (5 mg, 0.006 mmol), **S3** (1 mg, 0.012 mmol) and chlorobenzene (1 ml). The solution was heated at 100 °C, then 0.1 ml 9M acetic acid was added. The reaction was stirred at 100 °C for 1 hour. The solid was collected by filtration to afford S4 as a red solid. (6 mg ,99% yield). ^{1}H NMR (500 MHz, *o*-$C_6D_4Cl_2$) δ 10.59 (s, 2H), 10.49 (s, 2H), 9.75 (s, 2H), 9.31 (d, *J* = 8.6 Hz, 2H), 8.85 (s, 2H), 8.70 (d, *J* = 8.5 Hz, 2H), 7.38 (d, *J* = 5.2 Hz, 6H), 7.21 (d, *J* = 4.7 Hz, 4H), 5.65 (p, *J* = 8.5 Hz, 2H), 2.81 – 2.52 (m, 4H), 2.32 – 2.10 (m, 4H), 1.73 – 1.50 (m, 8H), 1.44 (q, *J* = 8.2 Hz, 8H), 1.31 (q, *J* = 7.3 Hz, 8H), 0.81 (t, *J* = 7.3 Hz, 12H). ^{13}C NMR could not be obtained due to poor solubility, structure was confirmed by mass spectroscopy and ^{1}H NMR. MALDI-TOF MS: m/z calculated for $C_{72}H_{68}N_4O_4$ [M$^-$]: 1052.5241; found: 1052.5375.

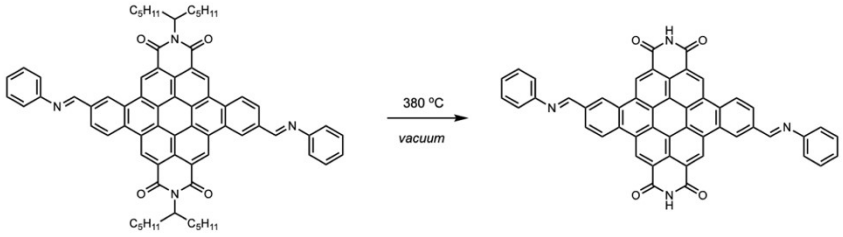

S4 S4-H

S4-H: A 4 ml vial charged with **S4** (1 mg) was placed in a borosilicate glass tube. The tube was then sealed under vacuum and transferred to a tube furnace. The end with the solid was placed in the middle of the furnace and the other end was out of the furnace. The furnace was heated to T = 380 ºC for 2 hours. After cooling to room temperature, **S4-H** was collected as an orange solid. MS: m/z $C_{50}H_{24}N_4O_4$ [M$^-$]: 744.1798; found:744.1748.

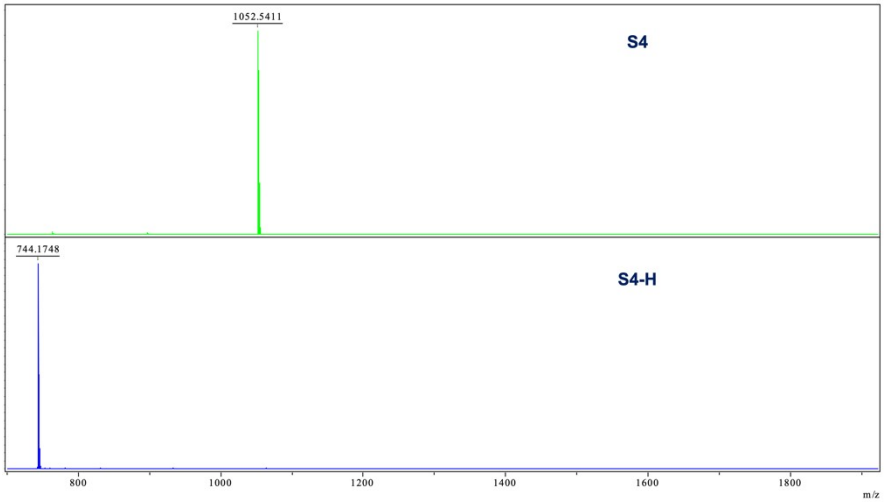

2.3 Synthesis of RA-2DPs

Imine-condensation:

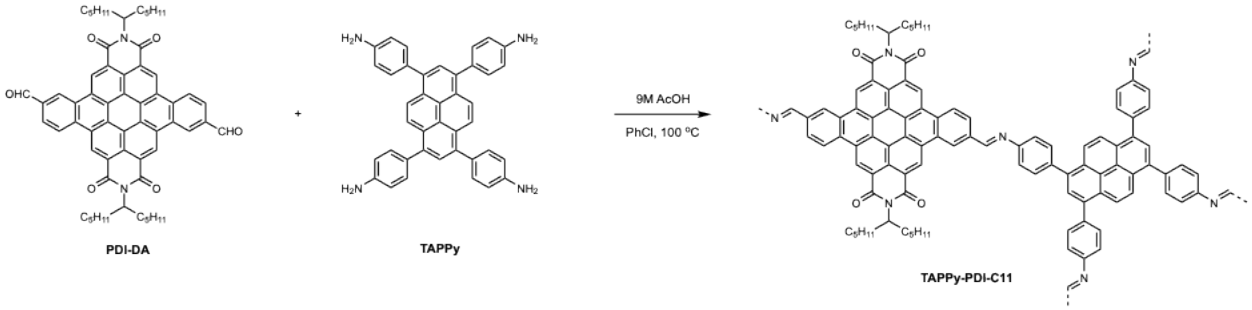

TAPPy-PDI-C11: To a vial was added **PDI-DA** (10 mg, 0.011 mmol), **TAPPy** (3.1 mg, 0.0055 mmol) and chlorobenzene (20 ml). The solution was heated at 100 °C, then 1 ml 9M acetic acid was added. The reaction was stirred at 100 °C for 16 hours. The solid was collected by filtration and then dried under gentle N2 flow to afford **TAPPy-PDI-C11** as a brown solid (12 mg ,94 % yield). Elemental Analysis: Calculated: C: 83.52%, H: 6.05%, N: 4.87%; found: C: 78.77%, H: 6.01%, N: 4.39%.

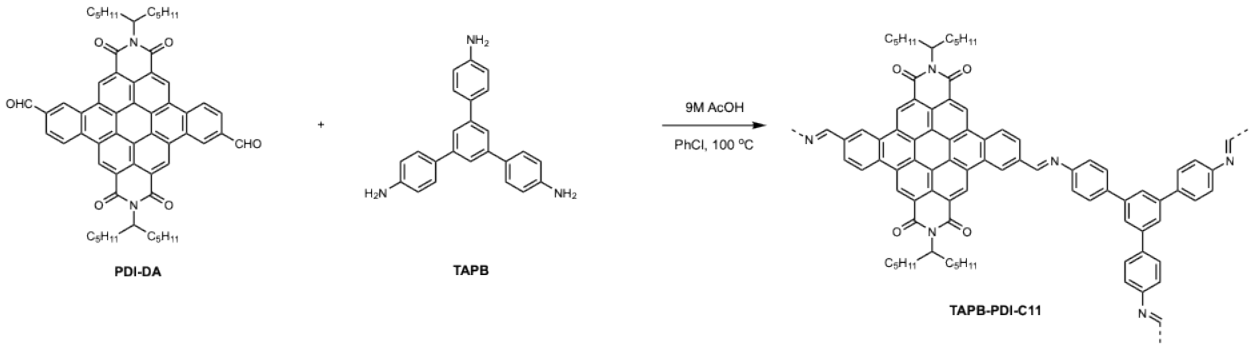

TAPB-PDI-C11: To a vial was added **PDI-DA** (10 mg, 0.011 mmol), **TAPB** (2.6 mg, 0.0074 mmol) and chlorobenzene (20 ml). The solution was heated at 100 °C, then 1 ml 9M acetic acid was added. The reaction was stirred at 100 °C for 16 hours. The solid was collected by filtration and then dried under gentle N2 flow to afford **TAPB-PDI-C11** as a red solid (11.7 mg, 96 % yield). Elemental Analysis: Calculated: C: 82.88%, H: 6.22%, N: 5.09%; found: C: 80.66%, H: 6.17%, N: 4.89%.

Thermolysis:

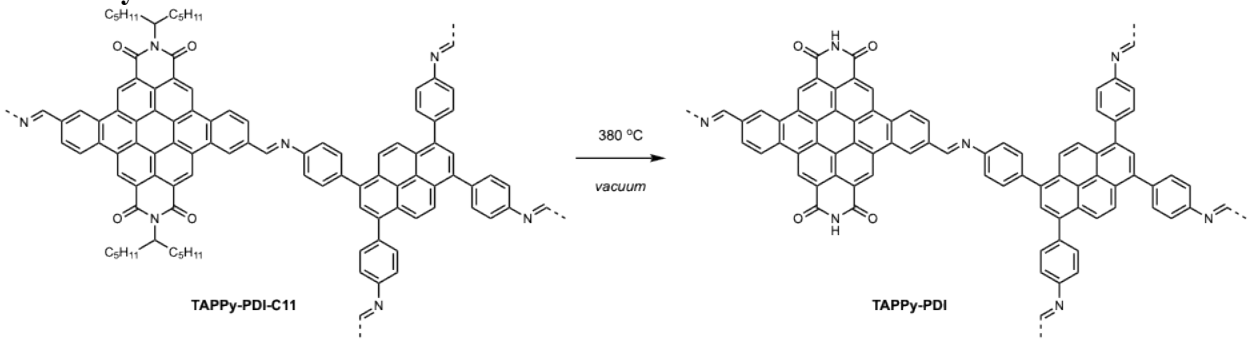

TAPPy-PDI: A 4 ml vial charged with **TAPPy-PDI-C11** (15 mg, 0.013 mmol) was placed in a borosilicate glass tube. The tube was then sealed under vacuum and transferred to a tube furnace. The end with the solid was placed in the middle of the furnace and the other end was out of the furnace. The furnace was heated to T = 380 ºC for 2 hours. After cooling to room temperature, **TAPPy-PDI** was collected as a black solid (11 mg, 99 % yield). Elemental Analysis: Calculated: C: 82.74%, H: 2.99%, N: 6.67%; found: C: 71.83%, H: 3.80%, N: 5.51%.

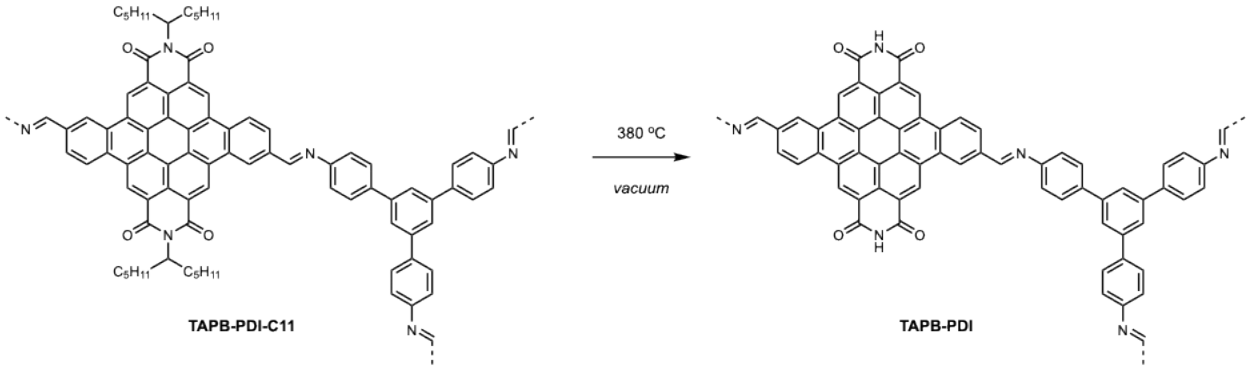

TAPB-PDI: A 4 ml vial charged with **TAPB-PDI-C11** (12 mg, 0.011 mmol) was placed in a borosilicate glass tube. The tube was then sealed under vacuum and transferred to a tube furnace. The end with the solid was placed in the middle of the furnace and the other end was out of the furnace. The furnace was heated to T = 380 ºC for 2 hours. After cooling to room temperature, **TAPB-PDI** was collected as a red solid (8.6 mg, 99 % yield). Elemental Analysis: Calculated: C: 81.81%, H: 3.05%, N: 7.07%; found: C: 71.67%, H: 3.91%, N: 6.01%.

3. Supporting Figures

3.1 Thermogravimetric Analysis

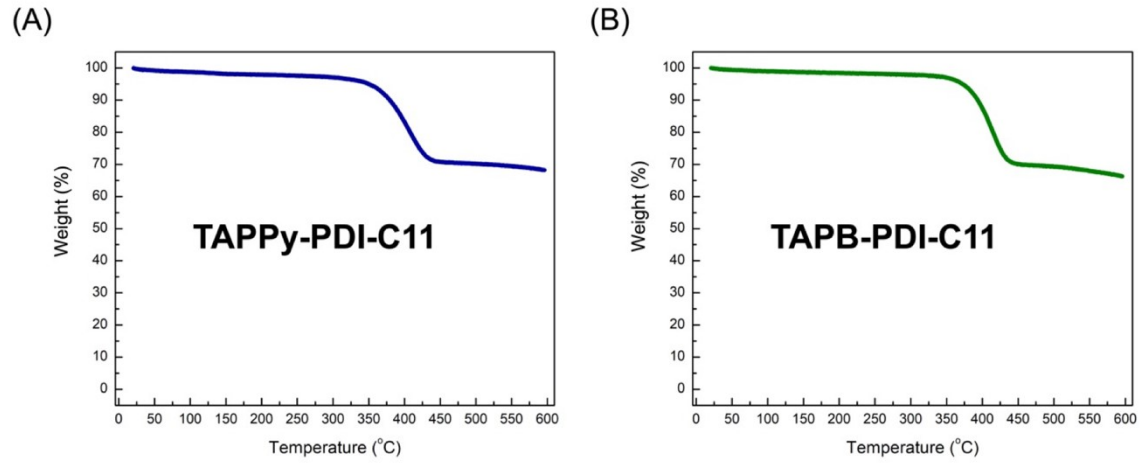

Figure S1. TGA of **TAPPy-PDI-C11** (A) and **TAPB-PDI-C11** (B).

3.2 FT-IR Spectra

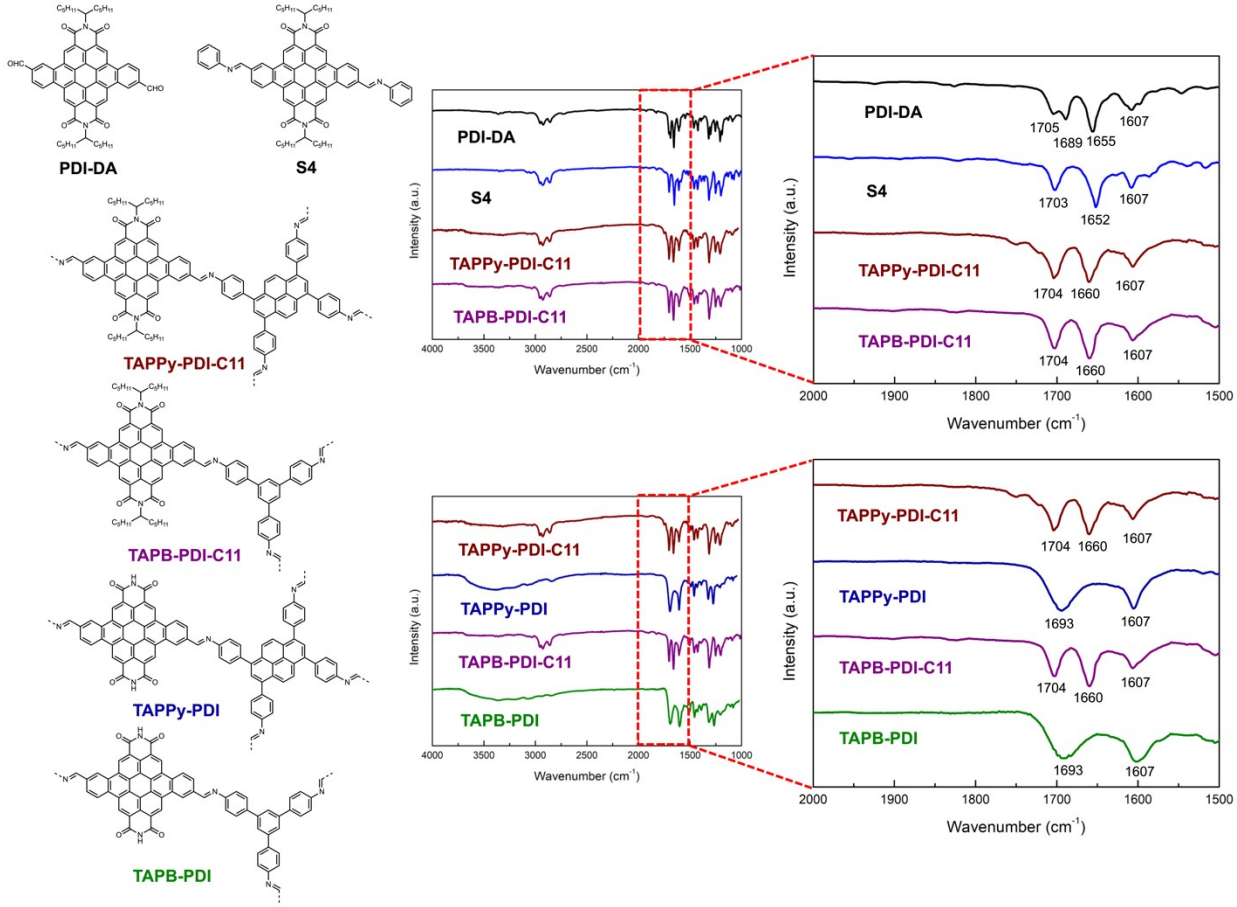

Figure S2. FT-IR spectra of **PDI-DA, S4 and RA-2DPs**.

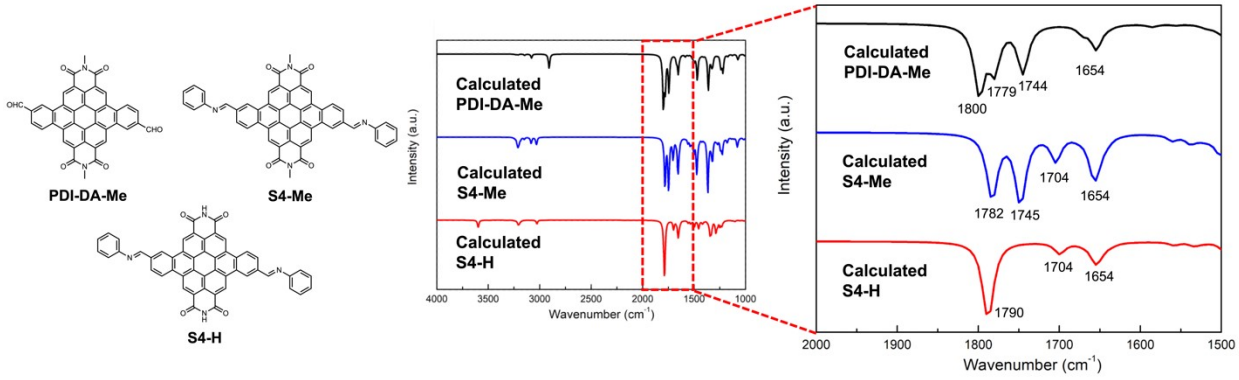

Figure S3. Calculated FT-IR spectra of the model compounds.

3.3 Simulation of X-ray Diffraction Patterns

Crystal modeling of the layered macromolecular sheets was carried out using Accelrys Materials Studio (ver.5.0). Initial structures were constructed by first estimating the primitive symmetry (*P*6 for TAPB-based 2DPs and *C2/m* for TAPPy-based 2DPs). In-plane (*a* and *b*) lattice parameters were estimated by approximating the distance between nodes of each topological network. The *c* parameter was estimated to be 4 Å, which is slightly larger than the interlayer spacing of graphite to accommodate the torsional flexibility of this structure. Backgrounds were removed via the Reflex module with a polynomial approximation with 30 iterations and an averaging window size of 0.9°. This protocol revealed a well-resolved peak that was initially obscured by air scatter that is known to be intense in the experimental measurement geometry. These structures were then optimized using a Geometry Optimization routine including energy minimization with cell parameters optimization, using the parameters from the Universal Force Field. Calculation of the simulated powder diffraction patterns and Pawley refinements were performed in the Materials Studio Reflex Plus Module using a Bragg-Brentano geometry with copper Kα radiation. Pawley refinement was conducted with peak profiles using the Pseudo-Voigt peak shape function and asymmetry was corrected using the Berar-Baldinozzi function. Crystallite size was then estimated by the LeBail method, which was Pawley refined to the experimental data.

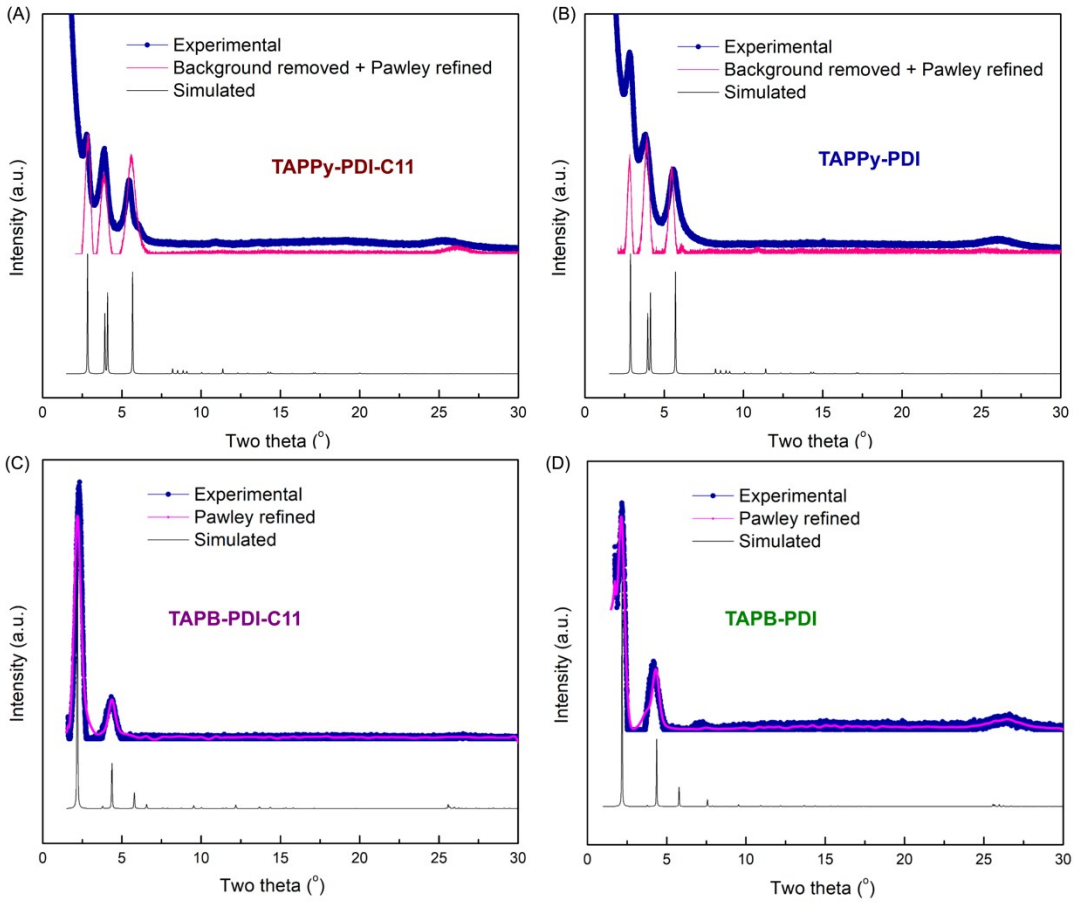

Figure S4. PXRD patterns for **TAPPy-PDI-C11** (A), **TAPPy-PDI** (B) **TAPB-PDI-C11** (C) and **TAPB-PDI** (D).

3.4 Scanning Electron Microscopy

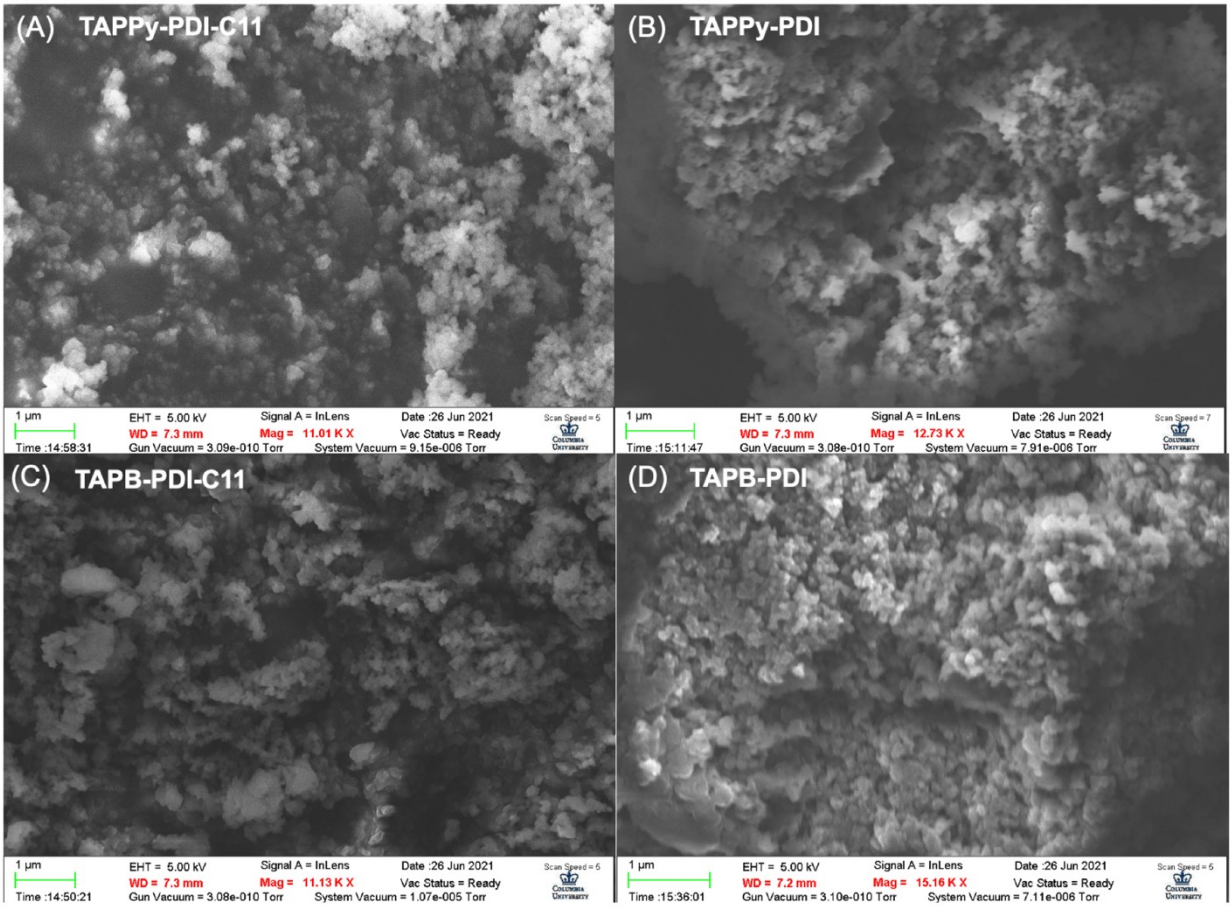

Figure S5. SEM images of **TAPPy-PDI-C11** (A), **TAPPy-PDI** (B), **TAPB-PDI-C11** (C) and **TAPB-PDI** (D).

3.5 BET surface area plots

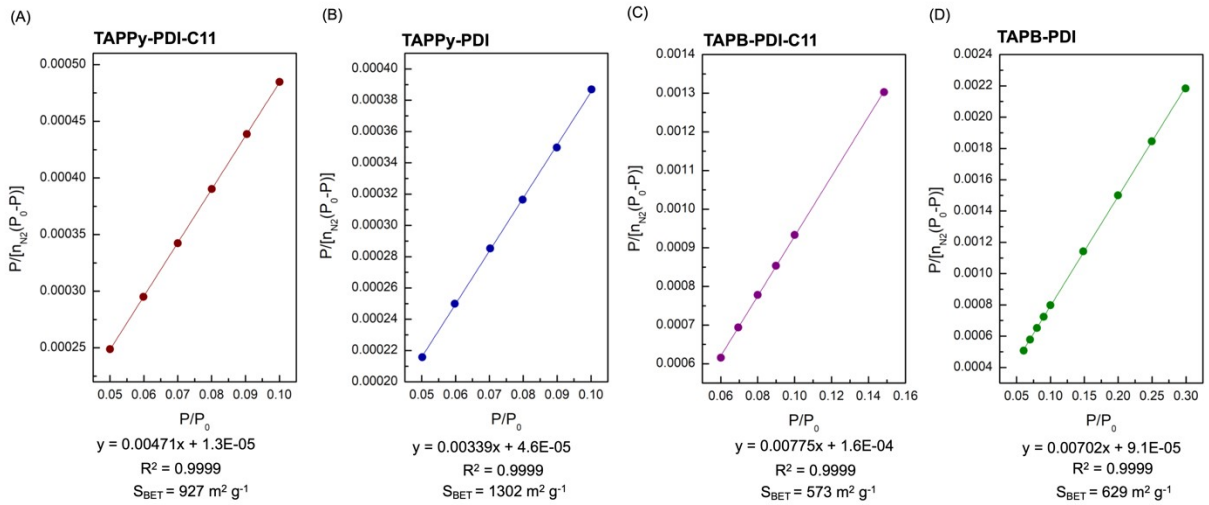

Figure S6. BET surface area plot for **TAPPy-PDI-C11** (A), **TAPPy-PDI** (B), **TAPB-PDI-C11** (C) and **TAPB-PDI** (D).

3.6 NMR spectra

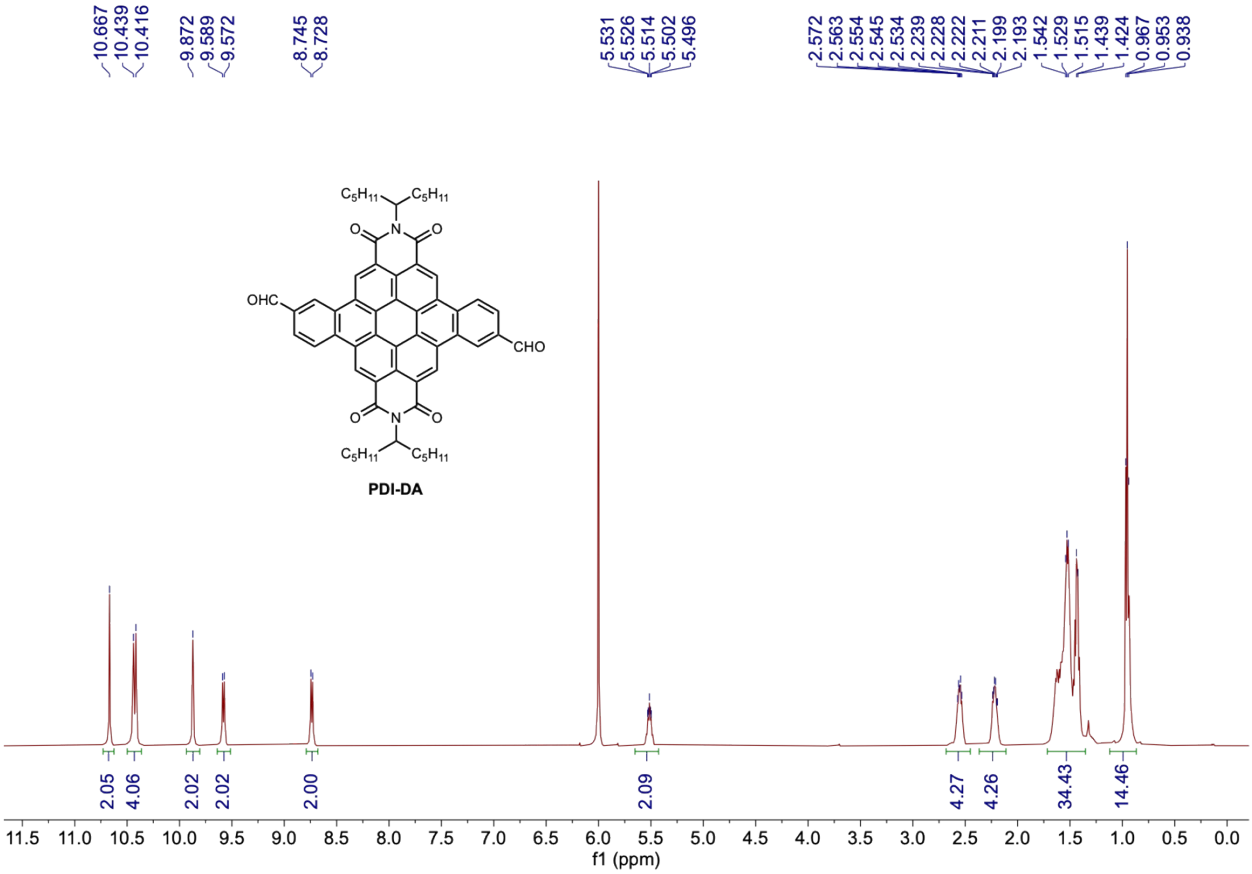

Figure S7. ^{1}H NMR (500 MHz, $C_2D_2Cl_4$) spectrum of **PDI-DA**.

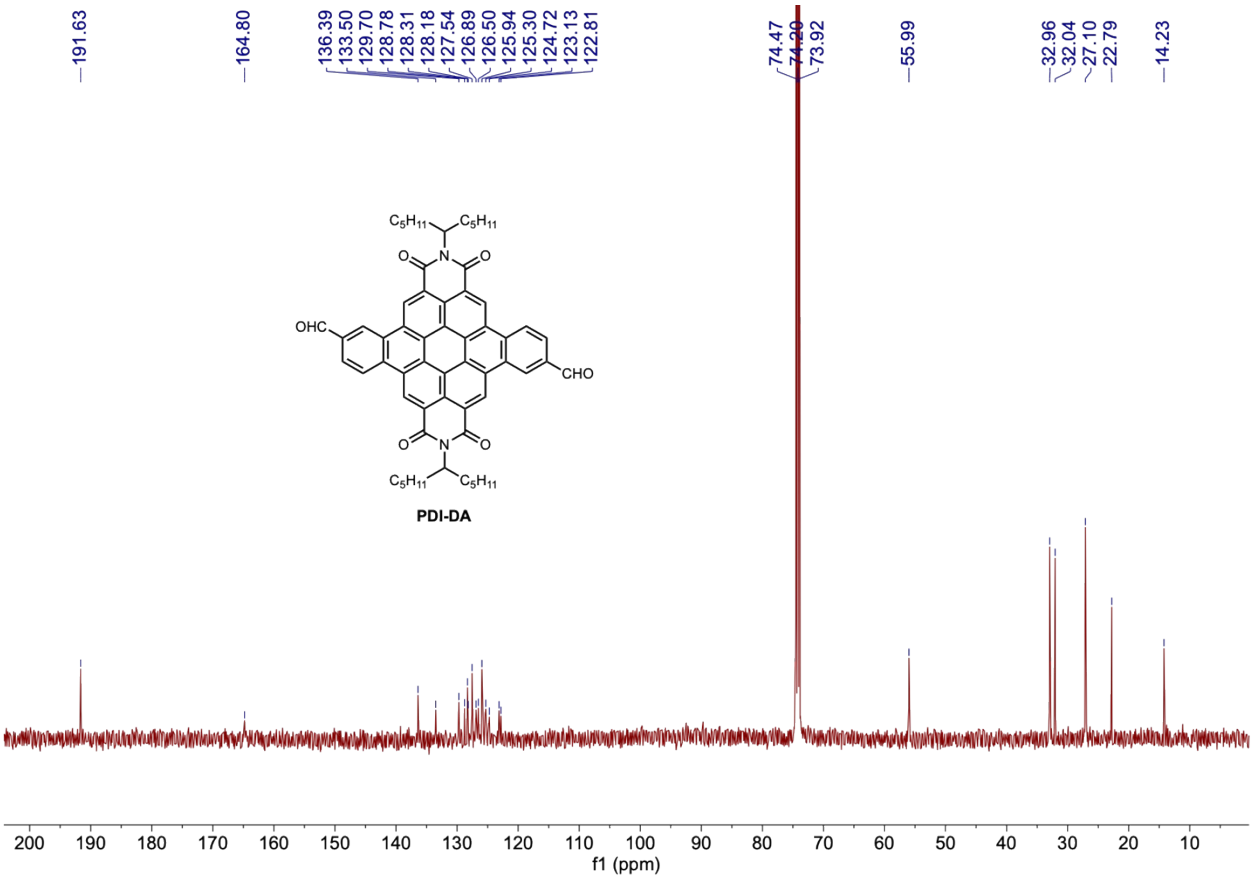

Figure S8. ^{13}C NMR (101 MHz, $C_2D_2Cl_4$) spectrum of **PDI-DA**.

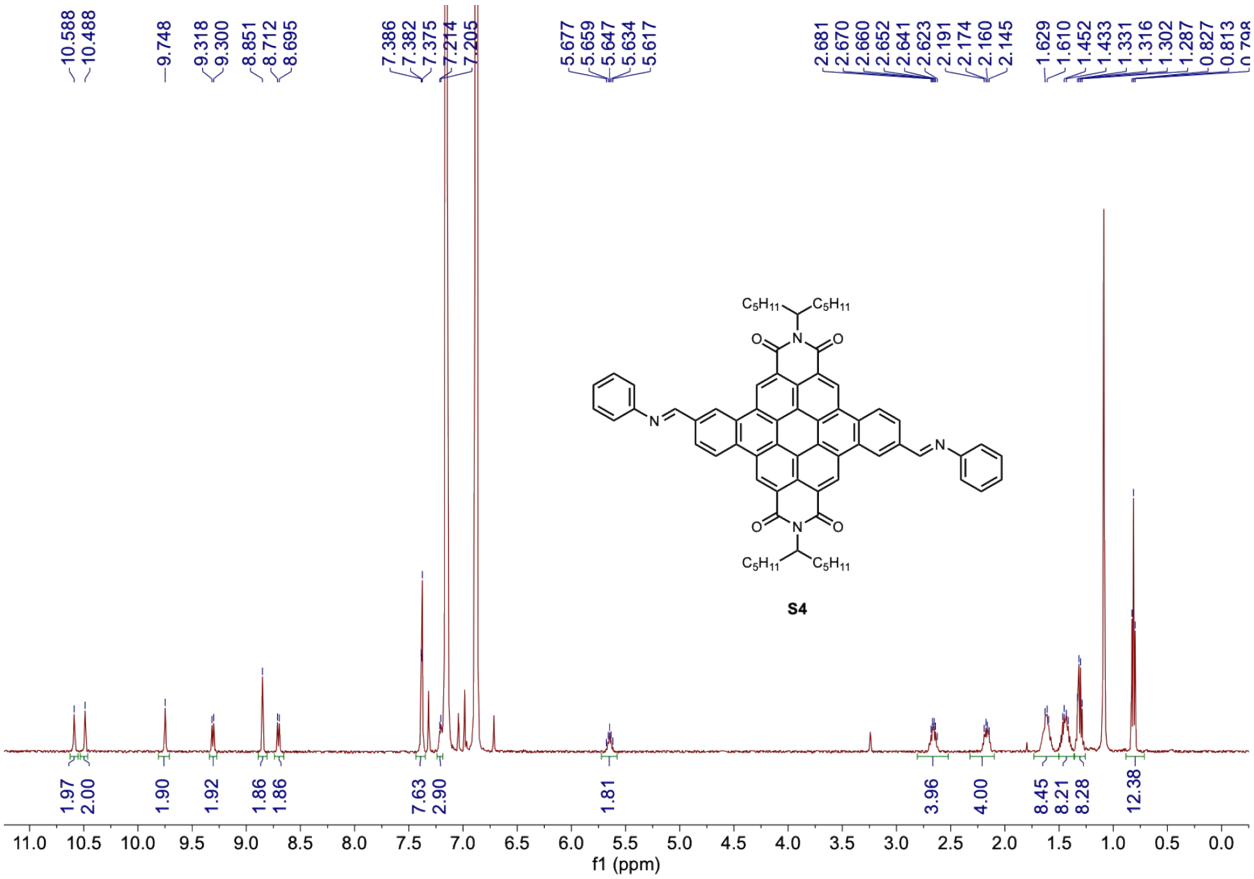

Figure S9. ^{1}H NMR (500 MHz, *o*-$C_6D_4Cl_2$) spectrum of **S4**.

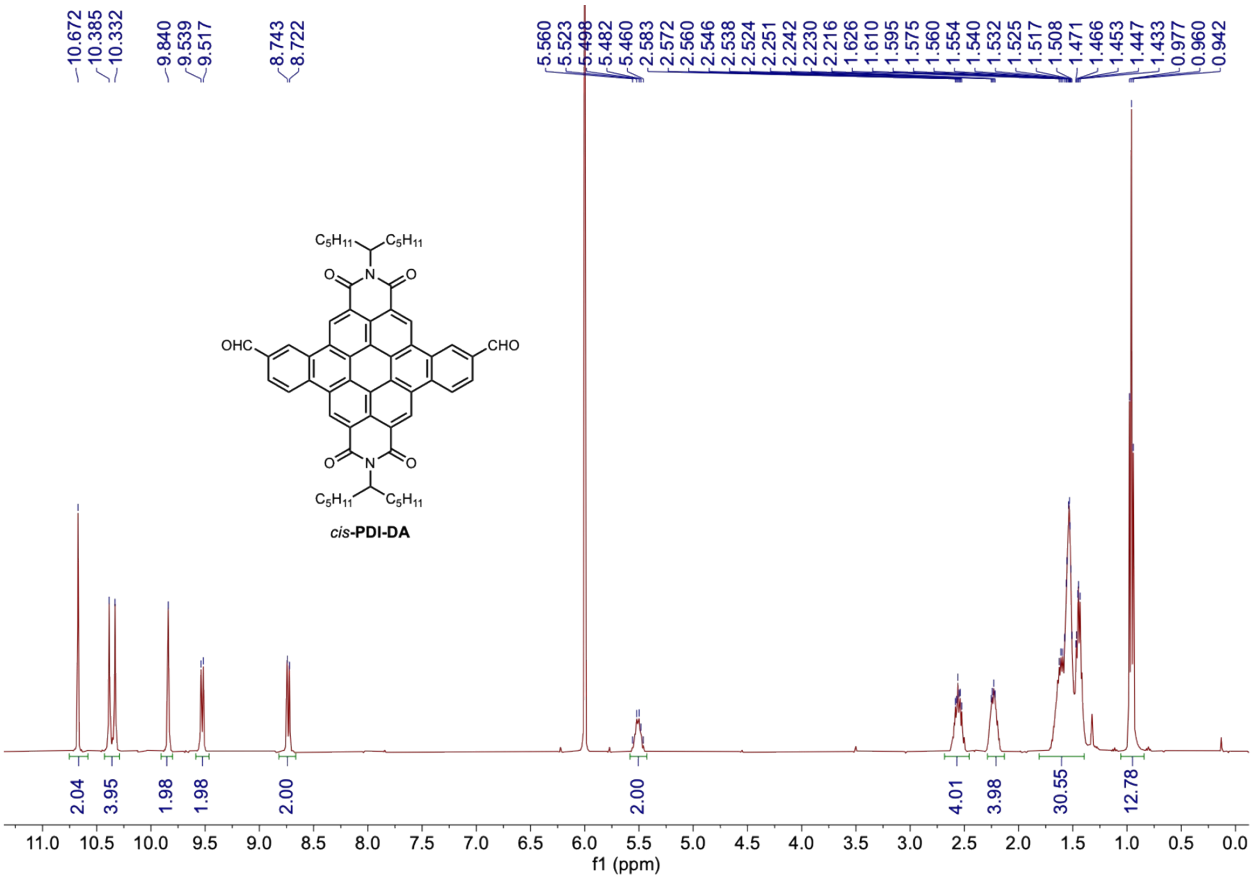

Figure S10. ^{1}H NMR (400 MHz, $C_2D_2Cl_4$) spectrum of *cis*-**PDI-DA**.

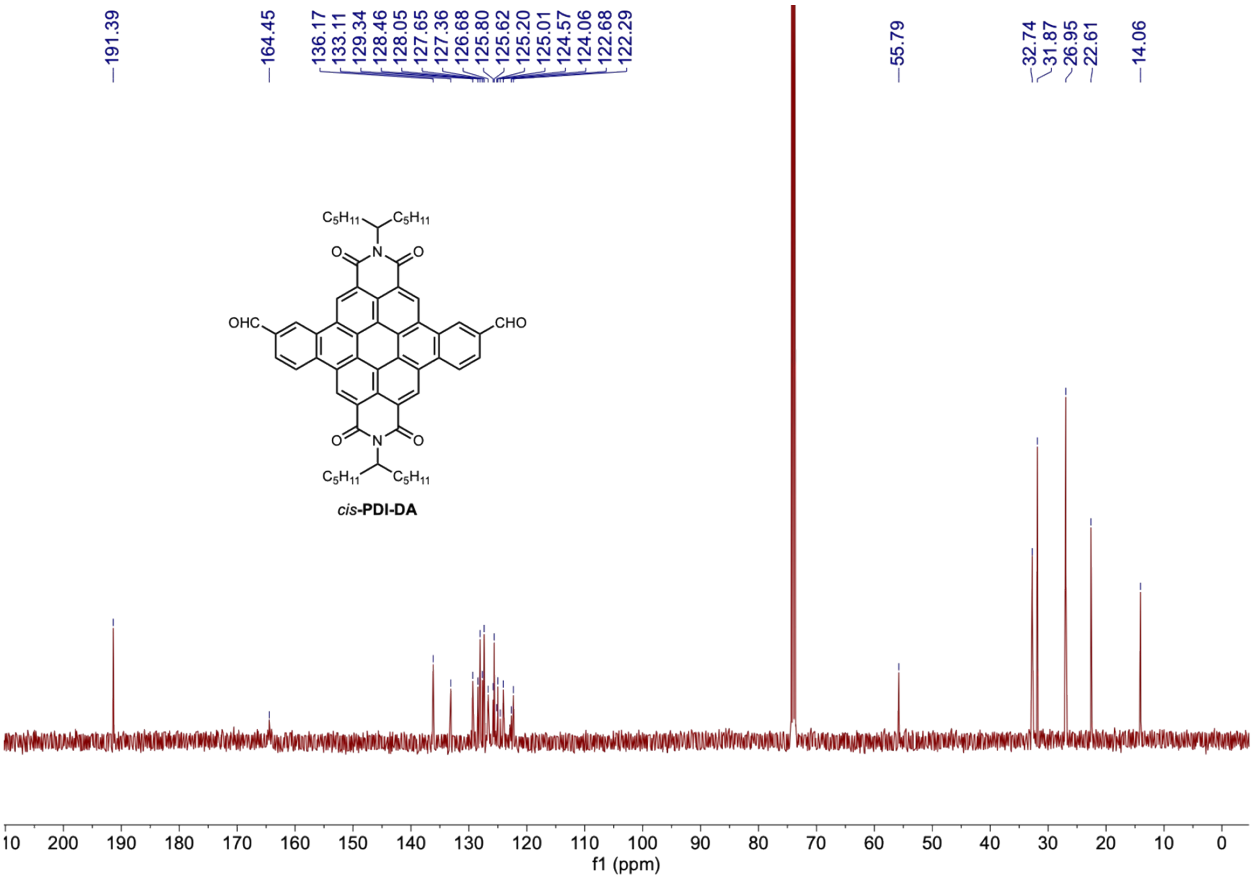

Figure S11. ^{13}C NMR (101 MHz, $C_2D_2Cl_4$) spectrum of *cis*-**PDI-DA**.

4. Electrochemical Data

4.1 Electrochemical Methods

Electrode Fabrication.

The active material was mixed with Super P carbon (C65, Imerys Graphite & Carbon), and poly(vinylidene fluoride) (PVDF) (Kynar Flex) in a 7:2:1 ratio. N-methyl-2-pyrrolidone (NMP) was added to the mixture and the slurry was sonicated for 2 h. After all materials are fully mixed, the slurry is drop-casted onto a carbon paper current collector (Fuel Cell Store). The coated electrode was dried for 2 h at 60 °C, and then dried in a vacuum oven at 110 °C overnight. The average active material loading was ~1 mg cm^{-2} for the performance tests and 5 mg cm^{-2} for the power tests.

Coin Cell Assembly.

In an argon-filled glovebox, the CR 2032 coin cells were assembled using lithium metal disks as anode, thin polyethylene separator (10 μm), 1M $LiPF_6$ in diethyl carbonate (DEC)/ethylene carbonate (EC) (1:1 vol) electrolyte (~100 μL) and the fabricated cathode.

Electrochemical Measurements.

All CV tests, EIS and GITT were conducted with a VMP3 multichannel potentiostat from Bio-Logic. After assembly of the coin cells, they were rested for 12 hours and then cycled for three times, and stopped at the voltage of 2.3 V, which is near its redox potential, then the cells were ready for electrochemical tests.

Determination of theoretical gravimetric capacity. Theoretical gravimetric capacities were calculated using Eq. 1:

$$C_{theor} = \frac{nF}{3.6 \times M_W} \qquad (1)$$

C_{theor} is the gravimetric theoretical capacity, n represents the number of electrons involved in the redox events of each repeating unit, F is the Faraday constant, M_w is the molar mass of the unit cell. The theoretical capacity of TAPPy-PDI is 63.7 mAh g^{-1} and the theoretical capacity of TAPB-PDI is 67.6 mAh g^{-1}.

Diffusion Coefficient Analysis. Cyclic voltammetry was performed on the assembled coin cells at scan rates between 1 mV s^{-1} to 25 mV s^{-1}. The peak current (i_p) from the oxidation peak of each scan was plotted versus the square root of scan rate (υ). The diffusion coefficient was determined from the slope using the Randles-Sevcik equation[2,3](Eq. 2):

$$i_p = 0.4463nFAC\left(\frac{nFvD}{RT}\right)^{\frac{1}{2}} \qquad (2)$$

Where *n* is the number of electrons involved in the redox events, *A* is the geometric electrode area, *C* is the concentration of the Li^+, *D* is the diffusion coefficient, F is the Faraday constant.

Electrochemical impedance spectroscopy (EIS). The amplitude for EIS is 10 mV and the frequency range is from 0.1 Hz to 1 MHz. Around 6 frequencies were taken in each decade and with a total measurement time of around 1 minute.

Galvanostatic intermittent titration technique (GITT). GITT analysis was performed on the coin cells at 25 mA/g discharging current of 10 minutes and followed by 10-minute rest, until the equilibrium voltage reached 1.4 V during the discharge process and 3.0 V during the charge process. The diffusion coefficient, D, can be estimated from the GITT data using the Eq. 3[4]:

$$D = \frac{4}{\pi \times \tau} \times \left(\frac{m \times \rho}{S}\right)^2 \times \left(\frac{\Delta V_s}{\Delta V_T}\right)^2 \quad (3)$$

where τ is the current pulse length, m is the mass of the active material on the electrode, ρ is the density of the active material, S is the interfacial area, ΔV_S is the change in steady-state potential after each current pulse and ΔV_T is the change in potential during the current pulse.

4.2 Supporting data of RA-2DPs

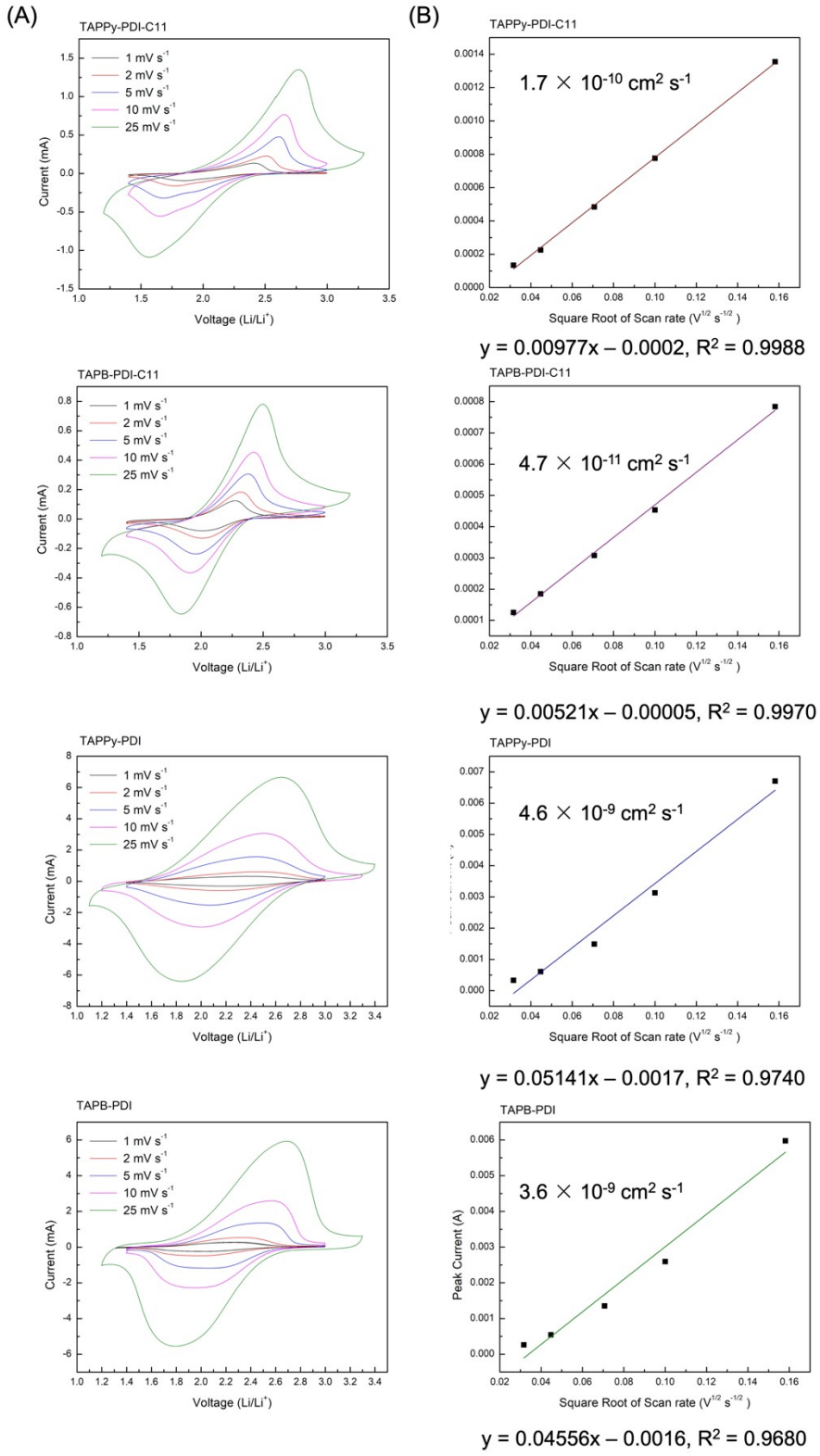

Figure S12. (A) CV profiles and (B) corresponding linear fits of the peak current vs. square root of scan rate of the four 2DPs at different scan rates.

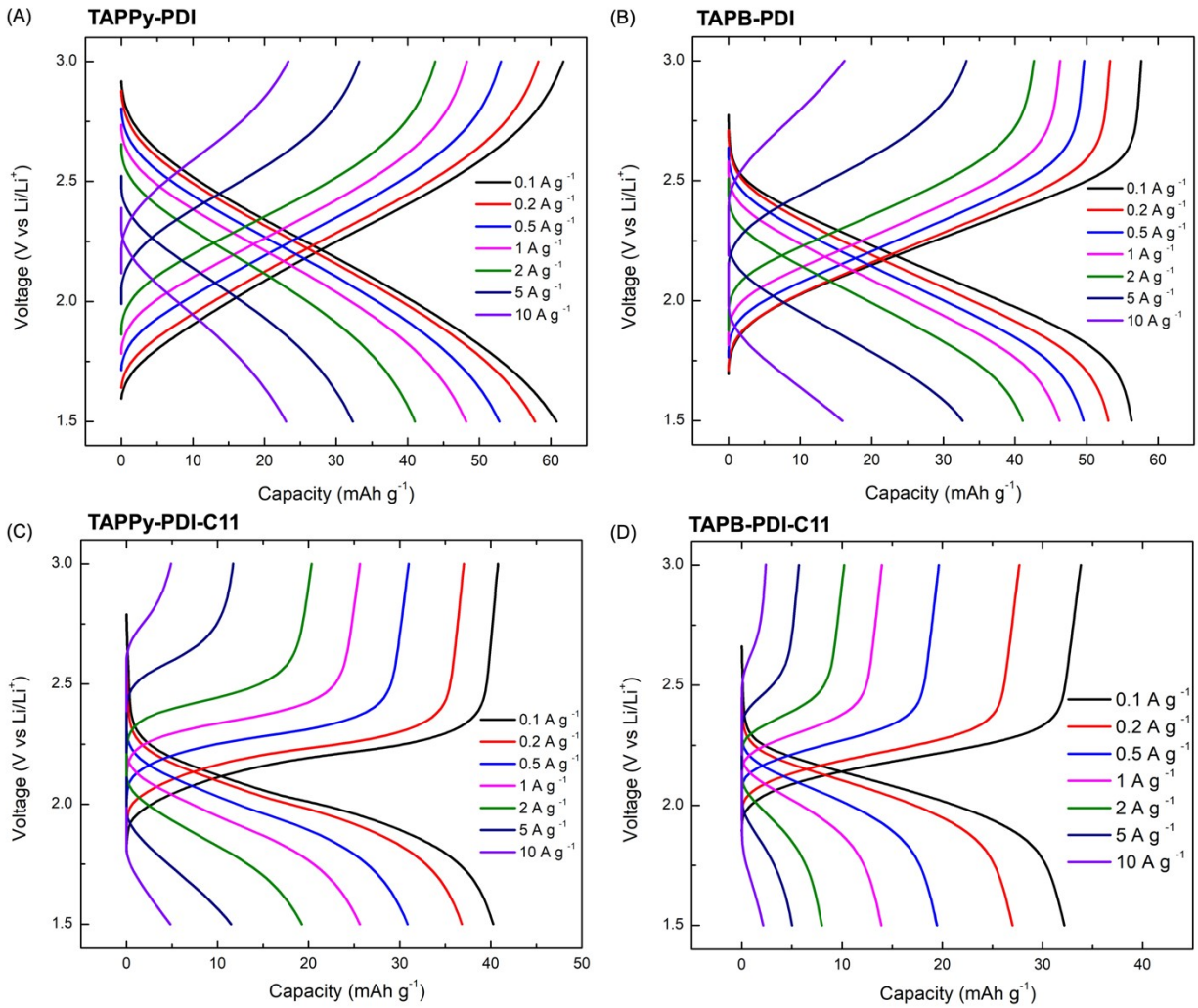

Figure S13. Charge/discharge curves of 2DPs at different charge/discharge rates.

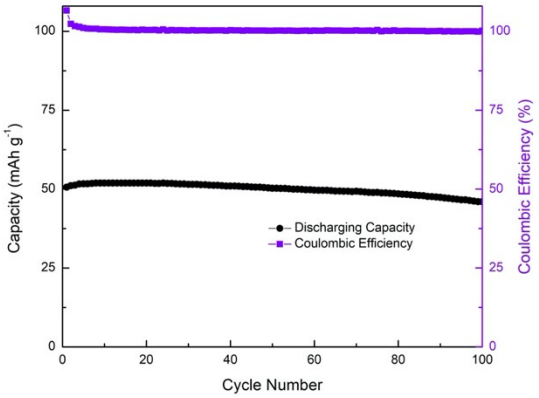

Figure S14. Cycling stability of **TAPPy-PDI** with 5 mg cm^{-2} loading cells at 0.2 A/g.

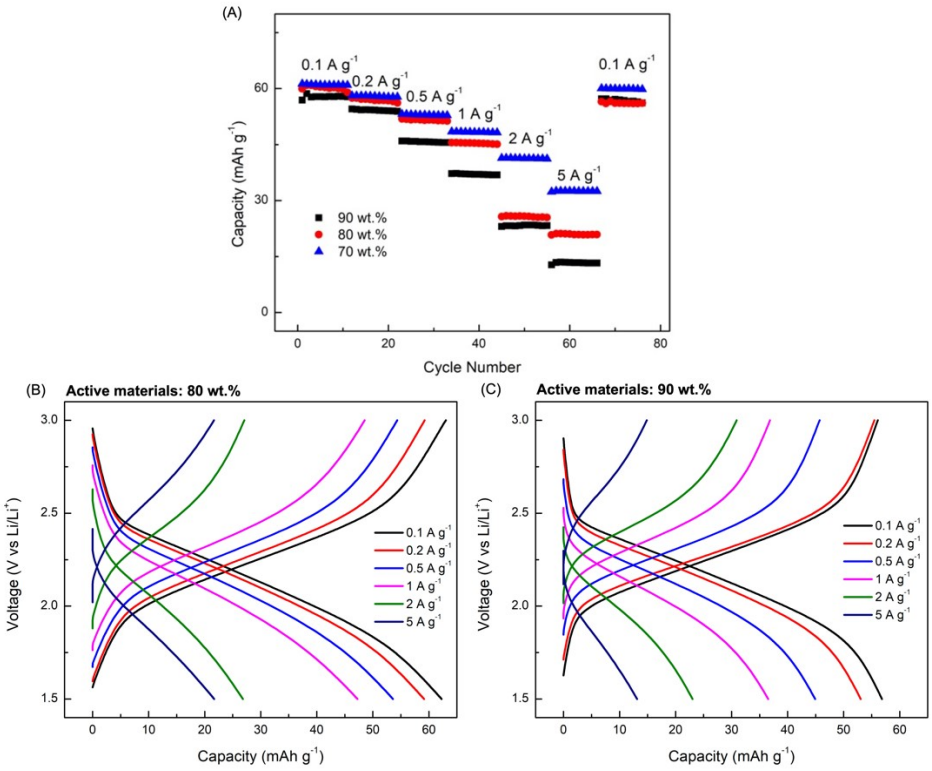

Figure S15. Rate performance of TAPPy-PDI with higher ratio of active materials.

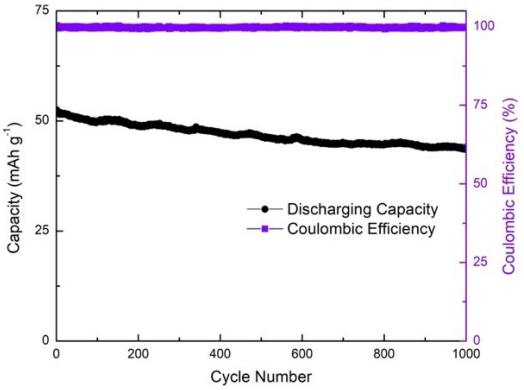

Figure S16. The cycling stability of battery with 80 wt.% active material loading of TAPPy-PDI, 10% of carbon and 10% of binder at 0.5 A/g over 1000 cycles.

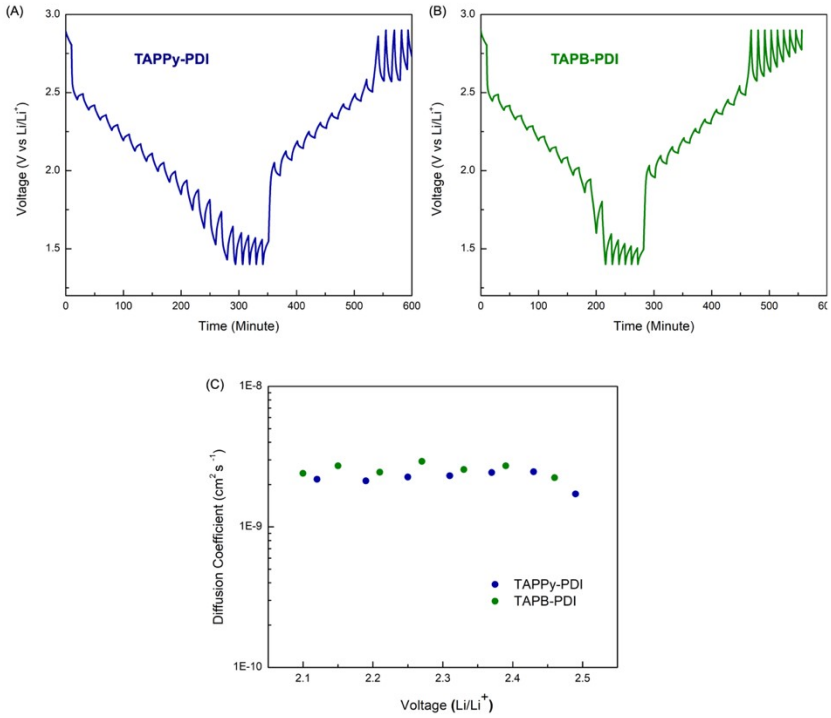

Figure S17. (A, B) GITT analysis and diffusion coefficients (C) of RA-2DPs.

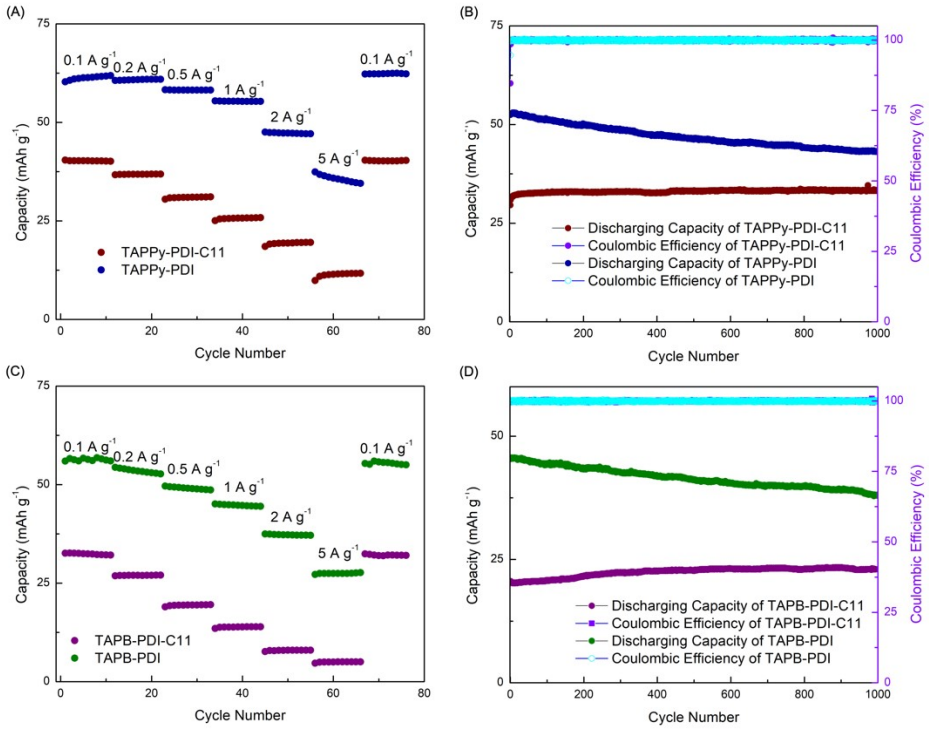

Figure S18. (A)-(B) The rate performance (A) and cycling stability (B) of TAPPy-PDI-C11 and TAPPy-PDI. (C)-(D). The rate performance (C) and cycling stability (D) of TAPB-PDI-C11 and TAPB-PDI.

Table S1. Battery performance comparison of TAPPy-PDI and TAPB-PDI with other reported 2DP cathodes.

Compound	Active ratio	Rate (percentage of theoretical)	Stability (Capacity retention (Discharge rate, cycle number))	Reference
TAPPy-PDI	70%	1.5C: 96% 80C: 55%	83% (7.5C, 1000)	**This work**
TAPB-PDI	70%	1.5C: 83% 80C: 44%	84% (7.5C, 1000)	**This work**
Tp–DANT-COF	60%	0.37C: 78% 7.5C: 63%	89.4% (3.7C, 200) 71.7%(7.5C, 600)	*J. Mater. Chem. A* **2016**, *4*, 18621
Tb–DANT-COF	60%	0.34C: 85% 3.4C: 74%	71% (1.4C, 100) 74% (3.4C, 300)	*J. Mater. Chem. A* **2016**, *4*, 18621
PIBN[a]	60%	0.1C: 87% 10C: 29%	N/A	*Angew. Chem. Int. Ed.* **2018**, *57*, 9443
2D-Pai[a]	80%	0.8C: 23%	100% (0.8C, 50)	*Adv. Mater.* **2019**, *31*, 1901478
PI-ECOF-1[a]	60%	0.1C: 79% 2C: 42% 5C: 0%	76% (1C, 300)	*Nanoscale* **2019**, *11*, 5330
BQ1-COF	50%	0.05C: 65% 10 C: 22%	81% (2C, 1000)	*Nano Energy* **2020**, *70*, 104498
DAPH-TFP COF	60%	0.5C: 48% 20C: 29%	50% (1C, 500)	*J. Am. Chem. Soc.* **2020**, *142*, 16
TAPB-NDI COF	60%	0.05C: 95% 5C: 16%	100% (2.5C, 400)	*ACS Appl. Energy Mater.* **2021**, *4*, 350

[a]The data of compounds incorporating with conductive reagents (Carbon nanotube, graphene, reduced graphene oxide) are not present.

Table S2. Summary of electrochemical values for 2DPs.

Compounds	**TAPPy-PDI**	**TAPB-PDI**	**TAPPy-PDI-C11**	**TAPB-PDI-C11**
Li+ diffusivity [$cm^2\ s^{-1}$]	4.6×10^{-9}	3.6×10^{-9}	1.7×10^{-10}	4.7×10^{-11}
Conductivity[a] [S/cm]	1.7×10^{-4}	1.2×10^{-4}	4.7×10^{-5}	3.3×10^{-5}
Capacity (1.5C) [mAh/g]	61	56	40	32
Capacity retention at 1000 cycles	83%	84%	99%	99%

[a]Electrical Conductivity of the composite, determined from EIS results.

4.3 Comparison of amorphous TAPPy-PDI

4.3.1 Synthesis of amorphous TAPPy-PDI

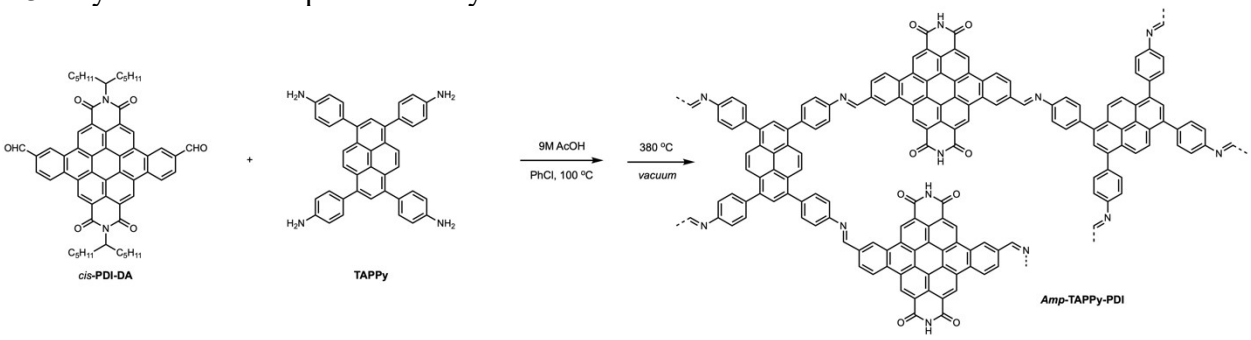

***Amp*-TAPPy-PDI:** To a vial was added *cis*-**PDI-DA** (10 mg, 0.011 mmol), **TAPPy** (3.1 mg, 0.0055 mmol) and chlorobenzene (20 ml). The solution was heated at 100 °C, then 1 ml 9M acetic acid was added. The reaction was stirred at 100 °C for 16 hours. The solid was collected by filtration and then dried under gentle N_2 flow. The brown solid was then transferred to a 4 ml vial. The vial was placed in a borosilicate glass tube, and then sealed under vacuum and transferred to a tube furnace. The end with the solid was placed in the middle of the furnace and the other end was out of the furnace. The furnace was heated to T = 380 ºC for 2 hours. After cooling to room temperature, ***Amp*-TAPPy-PDI** was collected as a black solid. (7 mg, 82% yield)

4.3.2 PXRD pattern of *Amp*-TAPPy-PDI

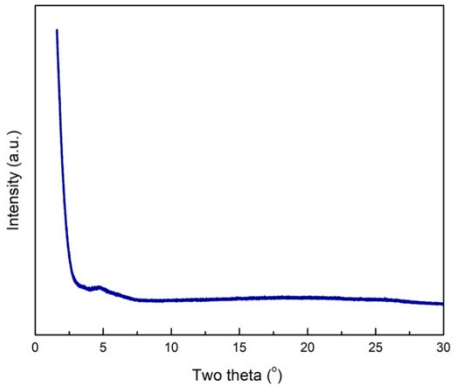

Figure S19. PXRD pattern of *Amp*-TAPPy-PDI.

4.3.3 Electrochemical analysis of *Amp*-TAPPy-PDI

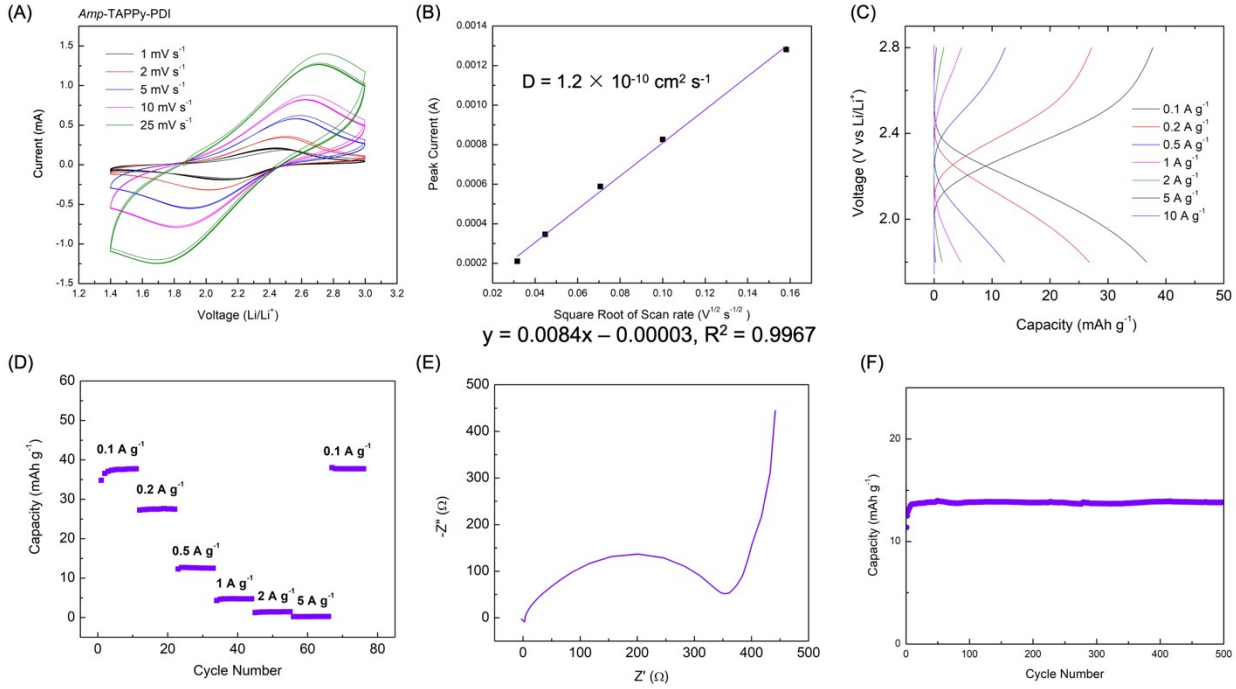

Figure S20. (A) CV profile, (B) corresponding linear fits of the peak current vs. square root of scan rate at different scan rates, (C) voltage profile, (D) rate performance and (E) EIS of *Amp*-TAPPy-PDI.

5. Calculation Details

Jaguar (version 8.2, Schrodinger, Inc., New York, NY, 2013) was used to perform all the quantum chemical calculations.[5] All geometries were optimized using the B3LYP functional and the 6-31G** basis set. In model compounds, the alkyl chain groups were replaced by methyl groups.

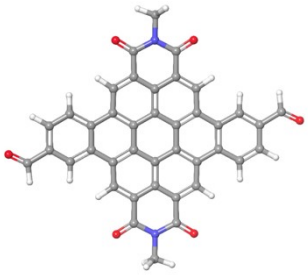

PDI-DA-Me

Total energy: -2096.188466 hartrees (B3LYP/6-31G**)

Final geometry:

C	6.0	-6.3947000000	-3.7409000000	-0.0124000000
C	6.0	-4.9655000000	-3.7191000000	-0.0089000000
C	6.0	-4.2521000000	-4.9424000000	-0.0087000000
C	6.0	-4.9582000000	-6.1686000000	-0.0119000000
C	6.0	-6.3351000000	-6.1779000000	-0.0156000000
C	6.0	-7.0895000000	-4.9788000000	-0.0161000000
C	6.0	-4.2394000000	-2.4877000000	-0.0055000000
C	6.0	-2.8216000000	-2.4961000000	-0.0024000000
C	6.0	-2.1485000000	-3.7416000000	-0.0023000000
C	6.0	-2.8378000000	-4.9328000000	-0.0053000000
C	6.0	-7.1143000000	-2.4990000000	-0.0119000000
C	6.0	-6.3877000000	-1.2675000000	-0.0079000000
C	6.0	-4.9586000000	-1.2456000000	-0.0050000000
C	6.0	-7.1003000000	-0.0435000000	-0.0067000000
C	6.0	-6.3946000000	1.1829000000	-0.0025000000
C	6.0	-5.0176000000	1.1920000000	-0.0001000000
C	6.0	-4.2639000000	-0.0075000000	-0.0013000000
C	6.0	-8.5322000000	-2.4912000000	-0.0150000000
C	6.0	-9.2045000000	-1.2453000000	-0.0134000000
C	6.0	-8.5148000000	-0.0540000000	-0.0093000000
C	6.0	-2.8083000000	0.0002000000	0.0013000000
C	6.0	-2.0965000000	-1.2349000000	0.0008000000
C	6.0	-2.0685000000	1.2117000000	0.0043000000
C	6.0	-0.6936000000	1.2177000000	0.0068000000
C	6.0	0.0121000000	-0.0034000000	0.0062000000
C	6.0	-0.6848000000	-1.1980000000	0.0032000000
C	6.0	-8.5452000000	-4.9874000000	-0.0205000000
C	6.0	-9.2577000000	-3.7531000000	-0.0199000000
C	6.0	-9.2845000000	-6.1990000000	-0.0258000000

C	6.0	-10.6594000000	-6.2056000000	-0.0303000000
C	6.0	-11.3658000000	-4.9850000000	-0.0297000000
C	6.0	-10.6694000000	-3.7900000000	-0.0245000000
C	6.0	1.4942000000	-0.0155000000	0.0085000000
C	6.0	-12.8479000000	-4.9741000000	-0.0348000000
O	8.0	-13.5380000000	-5.9744000000	-0.0398000000
O	8.0	2.1852000000	0.9843000000	0.0107000000
C	6.0	-2.0776000000	-6.2092000000	-0.0051000000
N	7.0	-2.8255000000	-7.3929000000	-0.0082000000
C	6.0	-4.2279000000	-7.4651000000	-0.0115000000
C	6.0	-9.2756000000	1.2220000000	-0.0075000000
N	7.0	-8.5281000000	2.4060000000	-0.0031000000
C	6.0	-7.1257000000	2.4790000000	-0.0005000000
O	8.0	-10.4982000000	1.2637000000	-0.0095000000
O	8.0	-6.5446000000	3.5550000000	0.0033000000
O	8.0	-4.8096000000	-8.5408000000	-0.0140000000
O	8.0	-0.8550000000	-6.2517000000	-0.0023000000
C	6.0	-2.0566000000	-8.6430000000	-0.0080000000
C	6.0	-9.2976000000	3.6557000000	-0.0011000000
H	1.0	-6.8142000000	-7.1476000000	-0.0179000000
H	1.0	-1.0684000000	-3.8069000000	0.0002000000
H	1.0	-4.5383000000	2.1614000000	0.0032000000
H	1.0	-10.2846000000	-1.1794000000	-0.0152000000
H	1.0	-2.5891000000	2.1605000000	0.0045000000
H	1.0	-0.1302000000	2.1447000000	0.0089000000
H	1.0	-0.1138000000	-2.1193000000	0.0026000000
H	1.0	-8.7636000000	-7.1477000000	-0.0265000000
H	1.0	-11.2221000000	-7.1330000000	-0.0346000000
H	1.0	-11.2406000000	-2.8687000000	-0.0243000000
H	1.0	1.9517000000	-1.0292000000	0.0080000000
H	1.0	-13.3061000000	-3.9607000000	-0.0336000000
H	1.0	-2.7642000000	-9.4680000000	-0.0106000000
H	1.0	-1.4160000000	-8.6820000000	-0.8914000000
H	1.0	-1.4201000000	-8.6841000000	0.8782000000
H	1.0	-8.5904000000	4.4810000000	0.0023000000
H	1.0	-9.9346000000	3.6978000000	-0.8869000000
H	1.0	-9.9376000000	3.6930000000	0.8827000000

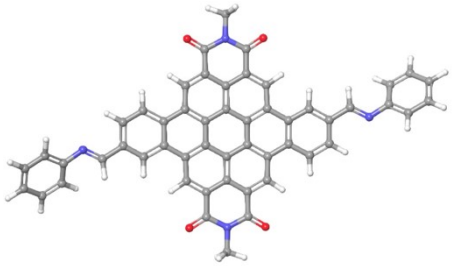

S4-Me

Total energy: -2518.564617 hartrees (B3LYP/6-31G**)

Final geometry:

C	6.0	-6.4196000000	3.7443000000	-0.1783000000
C	6.0	-4.9898000000	3.7556000000	-0.1890000000
C	6.0	-4.3046000000	4.9950000000	-0.1987000000
C	6.0	-5.0405000000	6.2038000000	-0.2001000000
C	6.0	-6.4176000000	6.1812000000	-0.1849000000
C	6.0	-7.1444000000	4.9656000000	-0.1701000000
C	6.0	-4.2352000000	2.5410000000	-0.1879000000
C	6.0	-2.8166000000	2.5803000000	-0.1841000000
C	6.0	-2.1734000000	3.8412000000	-0.1998000000
C	6.0	-2.8904000000	5.0168000000	-0.2085000000
C	6.0	-7.1113000000	2.4870000000	-0.1779000000
C	6.0	-6.3569000000	1.2726000000	-0.1928000000
C	6.0	-4.9276000000	1.2844000000	-0.1924000000
C	6.0	-7.0415000000	0.0328000000	-0.2054000000
C	6.0	-6.3056000000	-1.1757000000	-0.2202000000
C	6.0	-4.9291000000	-1.1524000000	-0.2158000000
C	6.0	-4.2036000000	0.0637000000	-0.1984000000
C	6.0	-8.5293000000	2.4466000000	-0.1653000000
C	6.0	-9.1723000000	1.1852000000	-0.1838000000
C	6.0	-8.4554000000	0.0098000000	-0.2047000000
C	6.0	-2.7503000000	0.0879000000	-0.1783000000
C	6.0	-2.0621000000	1.3351000000	-0.1639000000
C	6.0	-1.9840000000	-1.1062000000	-0.1625000000
C	6.0	-0.6112000000	-1.0847000000	-0.1248000000
C	6.0	0.0795000000	0.1481000000	-0.0975000000
C	6.0	-0.6502000000	1.3272000000	-0.1202000000
C	6.0	-8.5989000000	4.9402000000	-0.1403000000
C	6.0	-9.2840000000	3.6914000000	-0.1326000000
C	6.0	-9.3715000000	6.1309000000	-0.1095000000
C	6.0	-10.7455000000	6.1040000000	-0.0671000000
C	6.0	-11.4308000000	4.8676000000	-0.0498000000
C	6.0	-10.6946000000	3.6932000000	-0.0843000000
C	6.0	1.5449000000	0.1944000000	-0.0374000000
C	6.0	-12.8951000000	4.7966000000	0.0089000000

N	7.0	-13.6334000000	5.8421000000	0.0545000000
N	7.0	2.2536000000	-0.8718000000	-0.0014000000
C	6.0	-2.1610000000	6.3102000000	-0.2279000000
N	7.0	-2.9376000000	7.4761000000	-0.2299000000
C	6.0	-4.3417000000	7.5162000000	-0.2163000000
C	6.0	-9.1840000000	-1.2843000000	-0.2256000000
N	7.0	-8.4067000000	-2.4499000000	-0.2399000000
C	6.0	-7.0028000000	-2.4886000000	-0.2385000000
O	8.0	-10.4056000000	-1.3594000000	-0.2304000000
O	8.0	-6.3962000000	-3.5511000000	-0.2520000000
O	8.0	-4.9469000000	8.5794000000	-0.2186000000
O	8.0	-0.9394000000	6.3845000000	-0.2418000000
C	6.0	-2.1995000000	8.7437000000	-0.2477000000
C	6.0	-9.1431000000	-3.7184000000	-0.2583000000
C	6.0	3.6575000000	-0.7918000000	0.0099000000
C	6.0	-15.0345000000	5.7075000000	0.0613000000
C	6.0	4.3516000000	-1.7813000000	0.7239000000
C	6.0	5.7417000000	-1.7632000000	0.7816000000
C	6.0	6.4612000000	-0.7777000000	0.1017000000
C	6.0	5.7787000000	0.1891000000	-0.6382000000
C	6.0	4.3870000000	0.1873000000	-0.6868000000
C	6.0	-15.7709000000	6.6369000000	0.8121000000
C	6.0	-17.1590000000	6.5535000000	0.8695000000
C	6.0	-17.8366000000	5.5635000000	0.1532000000
C	6.0	-17.1121000000	4.6586000000	-0.6248000000
C	6.0	-15.7216000000	4.7252000000	-0.6733000000
H	1.0	-6.9199000000	7.1390000000	-0.1853000000
H	1.0	-1.0951000000	3.9303000000	-0.2084000000
H	1.0	-4.4267000000	-2.1099000000	-0.2257000000
H	1.0	-10.2505000000	1.0950000000	-0.1848000000
H	1.0	-2.4824000000	-2.0667000000	-0.1761000000
H	1.0	-0.0341000000	-2.0020000000	-0.1088000000
H	1.0	-0.1045000000	2.2630000000	-0.0957000000
H	1.0	-8.8765000000	7.0936000000	-0.1154000000
H	1.0	-11.3258000000	7.0196000000	-0.0406000000
H	1.0	-11.2358000000	2.7550000000	-0.0666000000
H	1.0	1.9917000000	1.1989000000	-0.0066000000
H	1.0	-13.3184000000	3.7816000000	0.0283000000
H	1.0	-2.9273000000	9.5511000000	-0.2479000000
H	1.0	-1.5538000000	8.8075000000	0.6306000000
H	1.0	-1.5701000000	8.7921000000	-1.1388000000
H	1.0	-8.4140000000	-4.5246000000	-0.2660000000
H	1.0	-9.7833000000	-3.7866000000	0.6237000000
H	1.0	-9.7776000000	-3.7647000000	-1.1458000000
H	1.0	3.7766000000	-2.5466000000	1.2354000000
H	1.0	6.2668000000	-2.5257000000	1.3497000000

H	1.0	7.5466000000	-0.7729000000	0.1354000000
H	1.0	6.3335000000	0.9433000000	-1.1891000000
H	1.0	3.8634000000	0.9212000000	-1.2921000000
H	1.0	-15.2303000000	7.4064000000	1.3538000000
H	1.0	-17.7157000000	7.2690000000	1.4679000000
H	1.0	-18.9205000000	5.5082000000	0.1881000000
H	1.0	-17.6326000000	3.9020000000	-1.2051000000
H	1.0	-15.1665000000	4.0401000000	-1.3070000000

S4-H

Total energy: -2518.564617 hartrees (B3LYP/6-31G**)

Final geometry:

C	6.0	-6.4274000000	3.7217000000	-0.1286000000
C	6.0	-4.9974000000	3.7413000000	-0.1627000000
C	6.0	-4.3183000000	4.9845000000	-0.2286000000
C	6.0	-5.0680000000	6.1888000000	-0.2608000000
C	6.0	-6.4430000000	6.1569000000	-0.2300000000
C	6.0	-7.1603000000	4.9377000000	-0.1641000000
C	6.0	-4.2392000000	2.5283000000	-0.1323000000
C	6.0	-2.8212000000	2.5710000000	-0.1710000000
C	6.0	-2.1826000000	3.8322000000	-0.2325000000
C	6.0	-2.9007000000	5.0056000000	-0.2605000000
C	6.0	-7.1133000000	2.4623000000	-0.0590000000
C	6.0	-6.3551000000	1.2493000000	-0.0257000000
C	6.0	-4.9253000000	1.2689000000	-0.0626000000
C	6.0	-7.0342000000	0.0063000000	0.0439000000
C	6.0	-6.2845000000	-1.1980000000	0.0776000000
C	6.0	-4.9098000000	-1.1661000000	0.0418000000
C	6.0	-4.1928000000	0.0528000000	-0.0298000000
C	6.0	-8.5313000000	2.4193000000	-0.0234000000
C	6.0	-9.1695000000	1.1584000000	0.0449000000
C	6.0	-8.4516000000	-0.0150000000	0.0780000000
C	6.0	-2.7403000000	0.0820000000	-0.0740000000
C	6.0	-2.0600000000	1.3309000000	-0.1467000000
C	6.0	-1.9670000000	-1.1078000000	-0.0502000000
C	6.0	-0.5942000000	-1.0802000000	-0.0964000000
C	6.0	0.0883000000	0.1554000000	-0.1733000000
C	6.0	-0.6486000000	1.3297000000	-0.1970000000
C	6.0	-8.6136000000	4.9077000000	-0.1312000000
C	6.0	-9.2936000000	3.6586000000	-0.0596000000
C	6.0	-9.3882000000	6.0963000000	-0.1693000000
C	6.0	-10.7615000000	6.0675000000	-0.1405000000
C	6.0	-11.4437000000	4.8317000000	-0.0670000000
C	6.0	-10.7057000000	3.6585000000	-0.0267000000
C	6.0	1.5534000000	0.2131000000	-0.2265000000
C	6.0	-12.9092000000	4.7715000000	-0.0380000000
N	7.0	-13.6326000000	5.8275000000	-0.0777000000
N	7.0	2.2745000000	-0.8451000000	-0.2094000000

C	6.0	-2.1713000000	6.2992000000	-0.3245000000
N	7.0	-2.9820000000	7.4328000000	-0.3535000000
C	6.0	-4.3746000000	7.5019000000	-0.3281000000
C	6.0	-9.1812000000	-1.3083000000	0.1486000000
N	7.0	-8.3703000000	-2.4417000000	0.1795000000
C	6.0	-6.9777000000	-2.5108000000	0.1505000000
O	8.0	-10.3979000000	-1.4094000000	0.1789000000
O	8.0	-6.4057000000	-3.5890000000	0.1835000000
O	8.0	-4.9466000000	8.5802000000	-0.3596000000
O	8.0	-0.9544000000	6.4005000000	-0.3512000000
C	6.0	3.6769000000	-0.7441000000	-0.2056000000
C	6.0	-15.0346000000	5.7229000000	-0.1080000000
C	6.0	4.3980000000	-1.7407000000	-0.8816000000
C	6.0	5.7882000000	-1.6998000000	-0.9188000000
C	6.0	6.4805000000	-0.6842000000	-0.2553000000
C	6.0	5.7707000000	0.2906000000	0.4475000000
C	6.0	4.3786000000	0.2662000000	0.4748000000
C	6.0	-15.7708000000	6.7239000000	0.5448000000
C	6.0	-17.1614000000	6.6808000000	0.5548000000
C	6.0	-17.8388000000	5.6582000000	-0.1134000000
C	6.0	-17.1136000000	4.6785000000	-0.7932000000
C	6.0	-15.7212000000	4.7053000000	-0.7931000000
H	1.0	-6.9521000000	7.1110000000	-0.2578000000
H	1.0	-1.1047000000	3.9238000000	-0.2588000000
H	1.0	-4.4009000000	-2.1201000000	0.0700000000
H	1.0	-10.2470000000	1.0680000000	0.0728000000
H	1.0	-2.4594000000	-2.0699000000	0.0056000000
H	1.0	-0.0110000000	-1.9940000000	-0.0779000000
H	1.0	-0.1080000000	2.2664000000	-0.2583000000
H	1.0	-8.8963000000	7.0588000000	-0.2244000000
H	1.0	-11.3453000000	6.9805000000	-0.1720000000
H	1.0	-11.2461000000	2.7213000000	0.0309000000
H	1.0	1.9903000000	1.2201000000	-0.2952000000
H	1.0	-13.3446000000	3.7639000000	0.0318000000
H	1.0	-2.4966000000	8.3221000000	-0.3984000000
H	1.0	-8.8556000000	-3.3310000000	0.2284000000
H	1.0	3.8440000000	-2.5296000000	-1.3804000000
H	1.0	6.3349000000	-2.4679000000	-1.4583000000
H	1.0	7.5660000000	-0.6616000000	-0.2726000000
H	1.0	6.3040000000	1.0688000000	0.9862000000
H	1.0	3.8329000000	1.0064000000	1.0521000000
H	1.0	-15.2282000000	7.5182000000	1.0474000000
H	1.0	-17.7200000000	7.4526000000	1.0763000000
H	1.0	-18.9244000000	5.6339000000	-0.1175000000
H	1.0	-17.6348000000	3.8946000000	-1.3354000000
H	1.0	-15.1633000000	3.9610000000	-1.3533000000

6. References

(1) Khokhlov, K.; Schuster, N. J.; Ng, F.; Nuckolls, C. Functionalized Helical Building Blocks for Nanoelectronics. *Org. Lett.* **2018**, *20* (7), 1991–1994.

(2) Randles, J. E. B. A Cathode Ray Polarograph. Part II.—The Current-Voltage Curves. *Trans. Faraday Soc.* **1948**, *44* (0), 327–338.

(3) Ševčík, A. Oscillographic Polarography with Periodical Triangular Voltage. *Collect. Czechoslov. Chem. Commun.* **1948**, *13*, 349–377.

(4) Shen, Z.; Cao, L.; Rahn, C. D.; Wang, C.-Y. Least Squares Galvanostatic Intermittent Titration Technique (LS-GITT) for Accurate Solid Phase Diffusivity Measurement. *J. Electrochem. Soc.* **2013**, *160* (10), A1842–A1846.

(5) Bochevarov, A. D.; Harder, E.; Hughes, T. F.; Greenwood, J. R.; Braden, D. A.; Philipp, D. M.; Rinaldo, D.; Halls, M. D.; Zhang, J.; Friesner, R. A., *Int. J. Quantum Chem.*, **2013**, *113*, 2110-2142.